Supporting Information

Ultrafast Formation of Porosity and Heterogeneous Structure on 2D oxides via Momentary Photothermal Effect

Ahrom Ryu†, Bo-In Park†, Hyun-Jae Lee, Jung-Won An, Jeong-Jun Kim, Sahn Nahm, Seong H. Kim, Byungju Lee, Ji-Won Choi* and Ji-Soo Jang**

A. Ryu, J.-W. Ahn, Dr. J.-S. Jang, Dr. J.W. Choi
Electronic Materials Research Center, Korea Institute of Science and Technology, Seongbuk-gu, Seoul 02792, Republic of Korea
E-mail: jwchoi@kist.re.kr, wkdwltn92@kist.re.kr

Dr. J.W. Choi
Division of Nano & Information Technology, KIST School, University of Science and Technology, Seoul 02792, Republic of Korea

Dr. H.-J. Lee, Dr. B. Lee
Computational Science Research Center, Korea Institute of Science and Technology, Seongbuk-gu, Seoul 02792, Republic of Korea
E-mail: blee89@kist.re.kr

J.-J. Kim
Department of Physics and Astronomy, Seoul National University, 1 Gwanak-ro, Gwanak-gu, Seoul, 08826, Korea

Seong H. Kim
Department of Chemical Engineering and Materials Research Institute, Pennsylvania State University, University Park, PA 16802, USA

A. Ryu, S. Nahm
Department of Material Science and Engineering, Korea University, Seoul 02841, Korea
Dr. B.-I Park
M.O.P. Materials, Seoul 07285, Republic of Korea

Keywords: 2D oxide, Formaldehyde, Chemical sensor, Flash-thermal shock

Supplementary data

Fig. S1 (a) The schematic of fabricating the Titania nanosheet film using drop coating method and (b) the photo of the sensor

Fig. S2. SEM images of layered (a) KTLO and (b) HTO powder

Fig. S3 Atomic force microscopy (AFM) images of Ti0.87O2 nanosheets and the corresponding (b) the thickness and (c) lateral size distribution

Fig. S4 The schematic of formation porous and reduced nanoparticles on surface of Ti0.87O2-x nanosheets

Fig. S5. The TEM-EDS analysis of the spherical Ti nanoparticles (Area 1 and 2, respectively) on the surface of FTS-Ti0.87O2

Fig. S6. TEM and FFT images of the samples. Top panel: Ti0.87O2, Bottom panel: FTS-Ti0.87O2 (a,e) TEM images (b,f) The fast Fourier transform pattern of the selected red box (c,g) The calculated d-spacing values from HR-TEM (d,h) The intensity profile showing an interlayer spacing between the monolayers in the nanosheets.

Fig. S7. EPR spectra of FTS-Ti0.87O2

Fig. S8 The survey XPS spectra of the 2D titania nanosheets.

Fig S9. (a) X-ray photoelectron spectroscopy (XPS) of pristine Ti0.87O2 nanosheets and (b) After FTS irradiation Ti0.87O2 nanosheets for Ti 2p and O 1s, respectively

Fig. S10. The UV-Vis analysis was conducted before and after FTS irradiation

Fig. S11 The Raman spectra of the pristine Ti0.87O2 and FTS-Ti0.87O2 samples

Fig. S12. The HCHO gas sensing properties under various FTS voltages (250, 300, 350, 400, 450 and 500 V).

Fig S13. (a) XRD analysis of $Ti_{0.87}O_2$ and FTS-$Ti_{0.87}O_2$, and (b) after cycle test conditions, respectively

Fig S14. SEM images of $Ti_{0.87}O_2$ and FTS-$Ti_{0.87}O_2$: (a, b) before and (c, d) after cycle test conditions

Fig. S15 Gas sensing properties of FTS-$Ti_{0.87}O_2$ of formaldehyde gas detection in various mixing gases (toluene, ammonia, formaldehyde)

Fig. S16. The photo of the sensing system in working condition.

Table S1. Comparison of the sensing performance of HCHO sensors at room temperature.

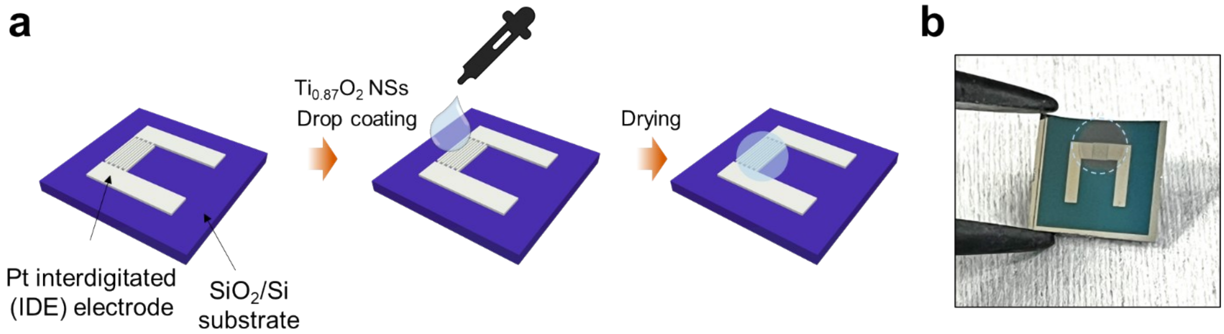

Fig. S1 (a) The schematic of fabricating the Titania nanosheet film using drop coating method and (b) the photo of the sensor

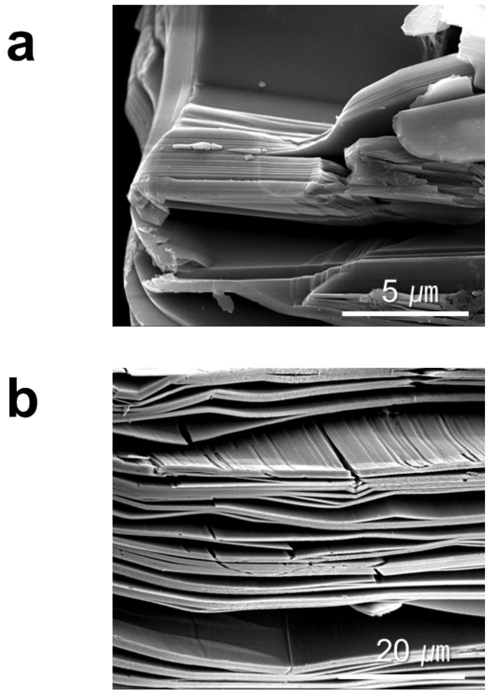

Fig. S2. SEM images of layered (a) KTLO and (b) HTO powder

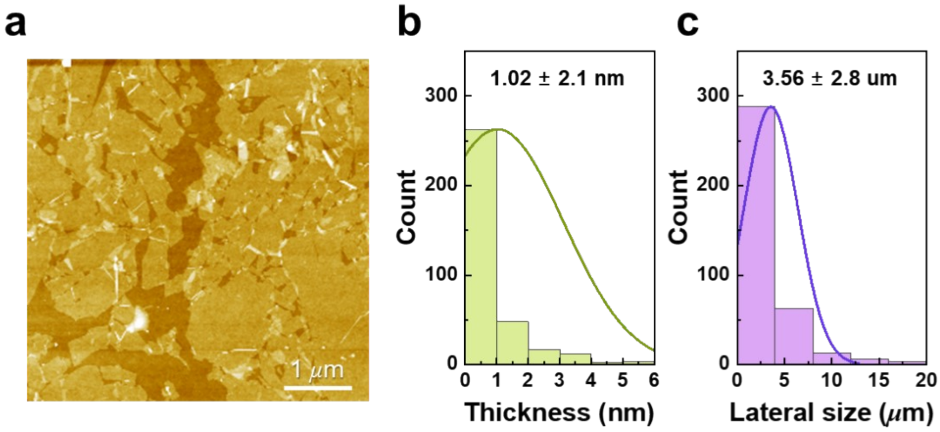

Fig. S3 Atomic force microscopy (AFM) images of $Ti_{0.87}O_2$ nanosheets and the corresponding (b) the thickness and (c) lateral size distribution

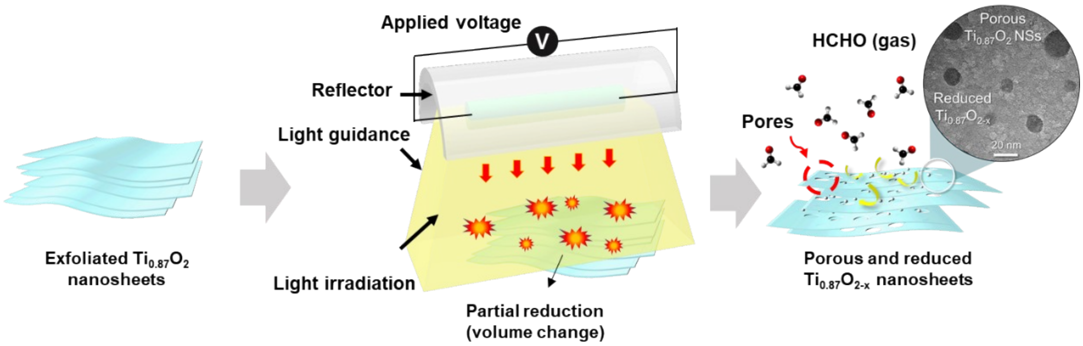

Fig. S4 The schematic of formation porous and reduced nanoparticles on surface of $Ti_{0.87}O_{2-x}$ nanosheets

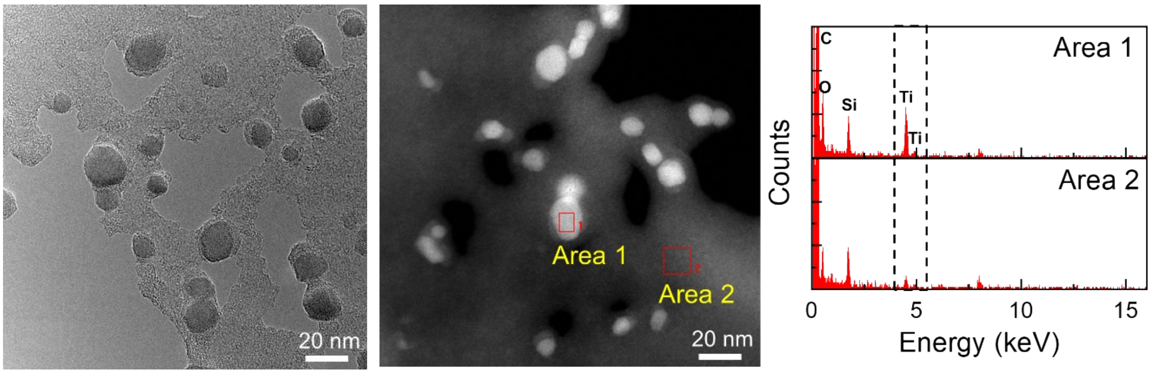

Fig. S5. The TEM-EDS analysis of the spherical Ti nanoparticles (Area 1 and 2, respectively) on the surface of FTS-$Ti_{0.87}O_2$

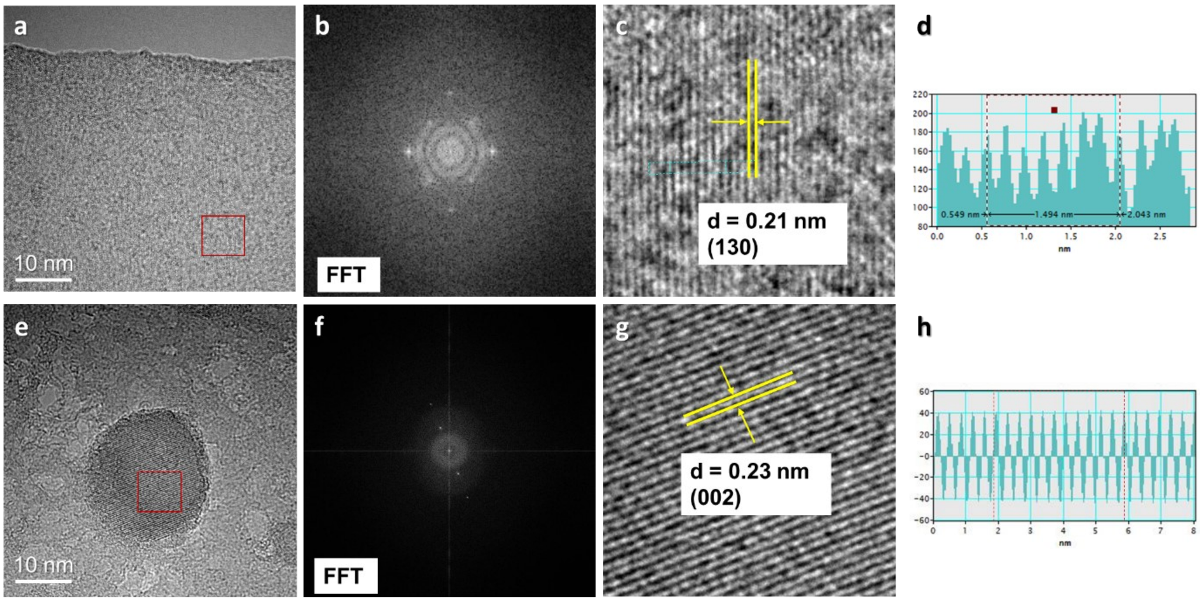

Fig. S6. TEM and FFT images of the samples. Top panel: $Ti_{0.87}O_2$, Bottom panel: FTS-$Ti_{0.87}O_2$ (a,e) TEM images (b,f) The fast Fourier transform pattern of the selected red box (c,g) The calculated d-spacing values from HR-TEM (d,h) The intensity profile showing an interlayer spacing between the monolayers in the nanosheets.

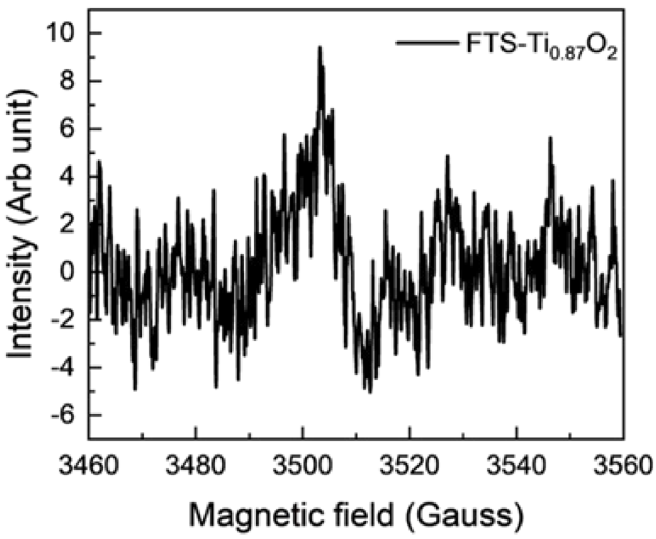

Fig. S7. EPR spectra of FTS-$Ti_{0.87}O_2$

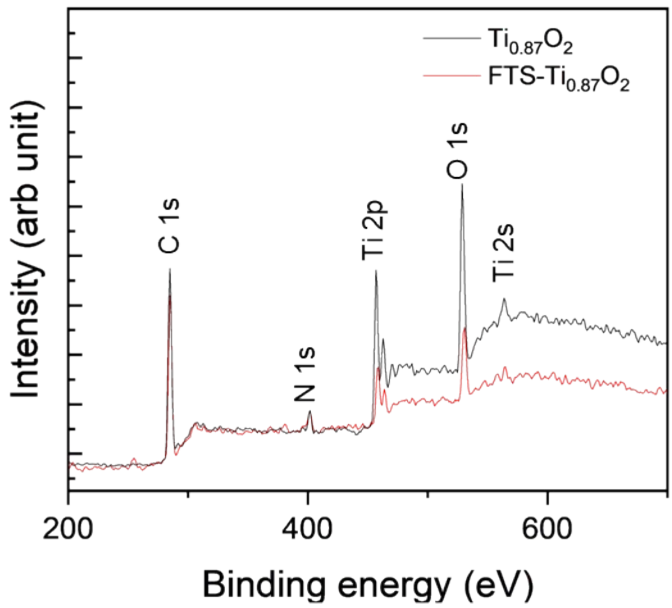

Fig. S8 The survey XPS spectra of the 2D titania nanosheets.

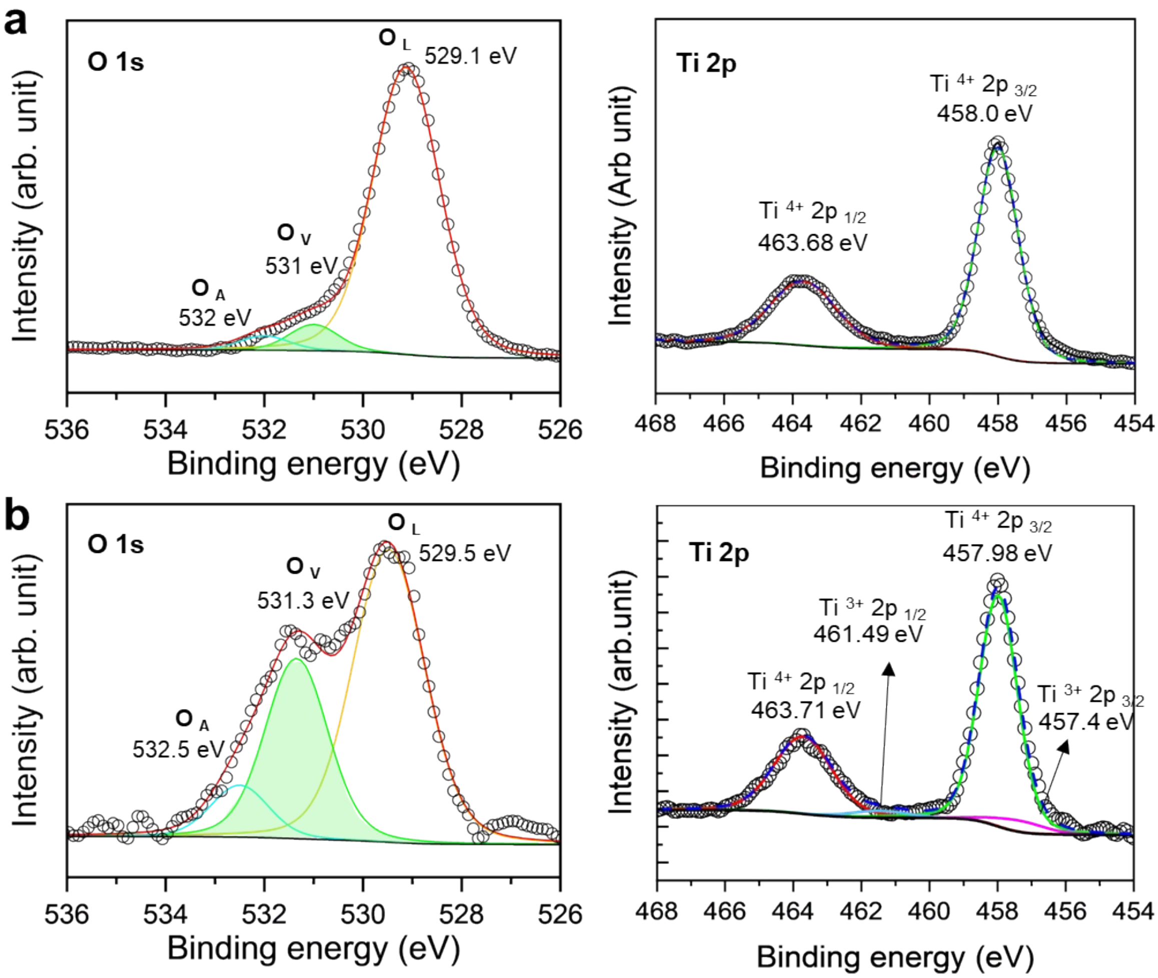

Fig S9. (a) X-ray photoelectron spectroscopy (XPS) of pristine $Ti_{0.87}O_2$ nanosheets and (b) After FTS irradiation $Ti_{0.87}O_2$ nanosheets for Ti 2p and O 1s, respectively

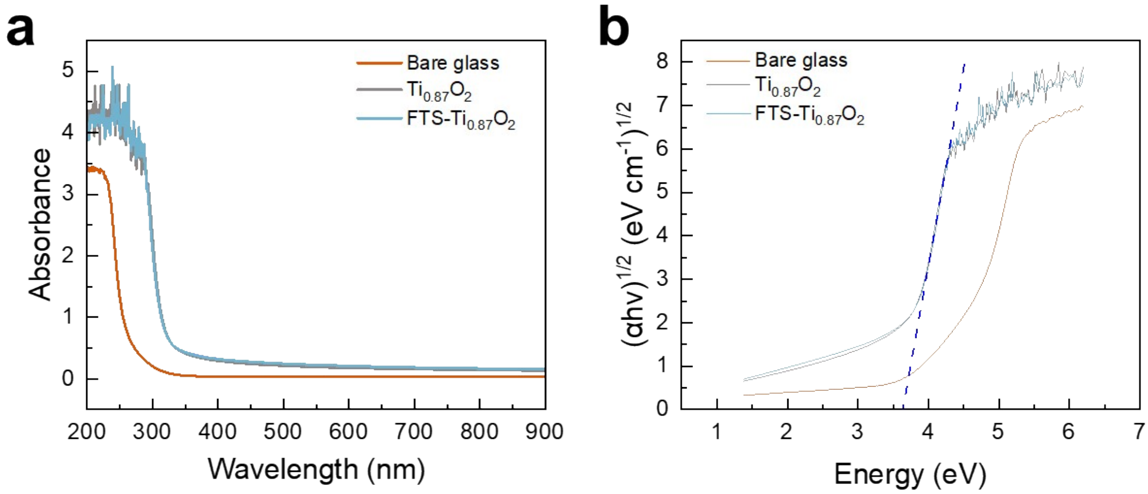

Fig. S10. The UV-Vis analysis was conducted before and after FTS irradiation

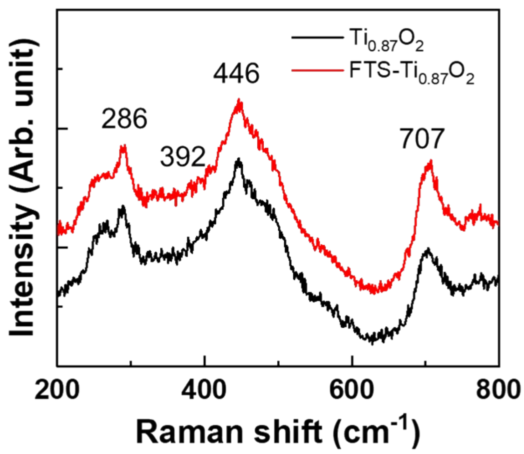

Fig. S11 The Raman spectra of the pristine $Ti_{0.87}O_2$ and FTS-$Ti_{0.87}O_2$ samples

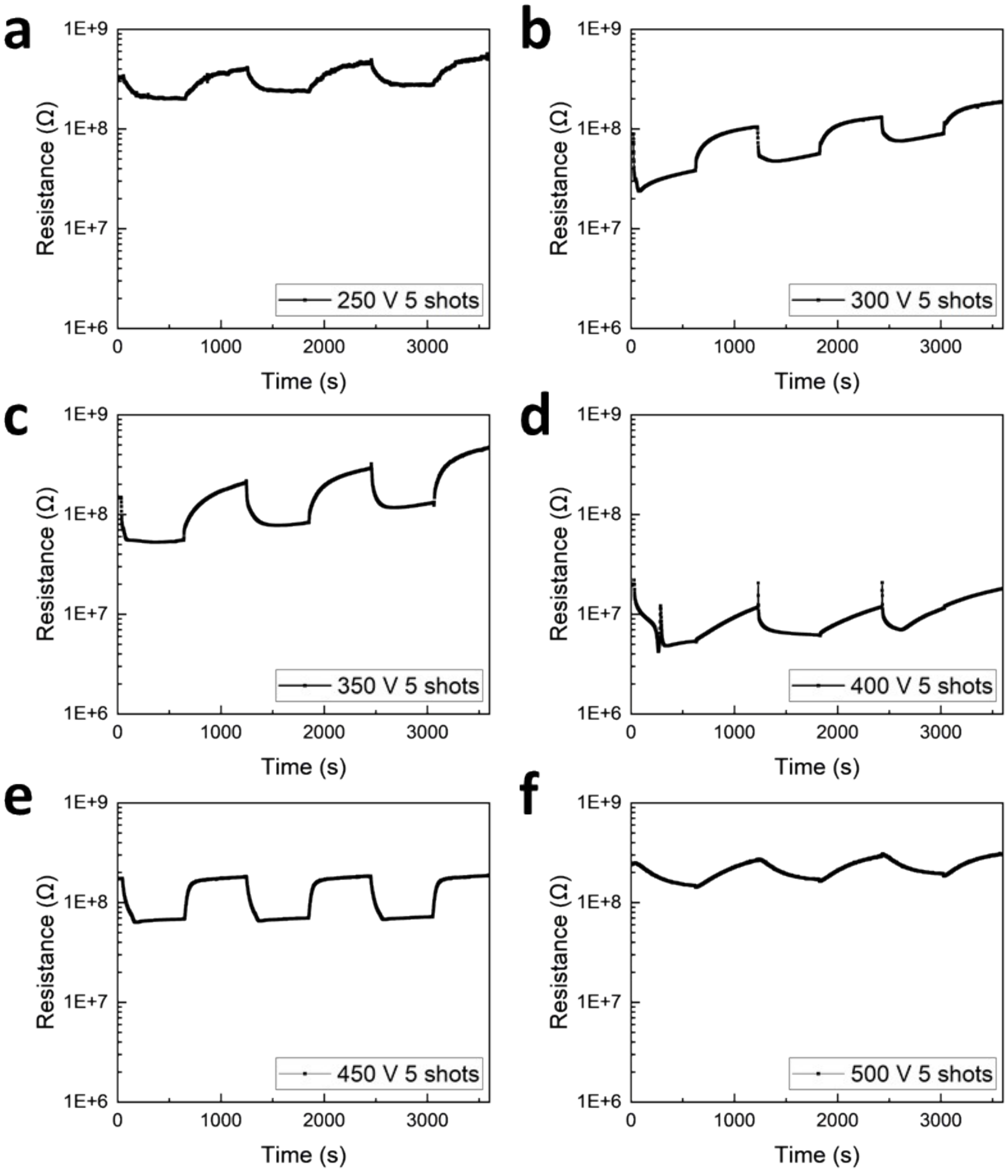

Fig. S12. The HCHO gas sensing properties under various FTS voltages (250, 300, 350, 400, 450 and 500 V).

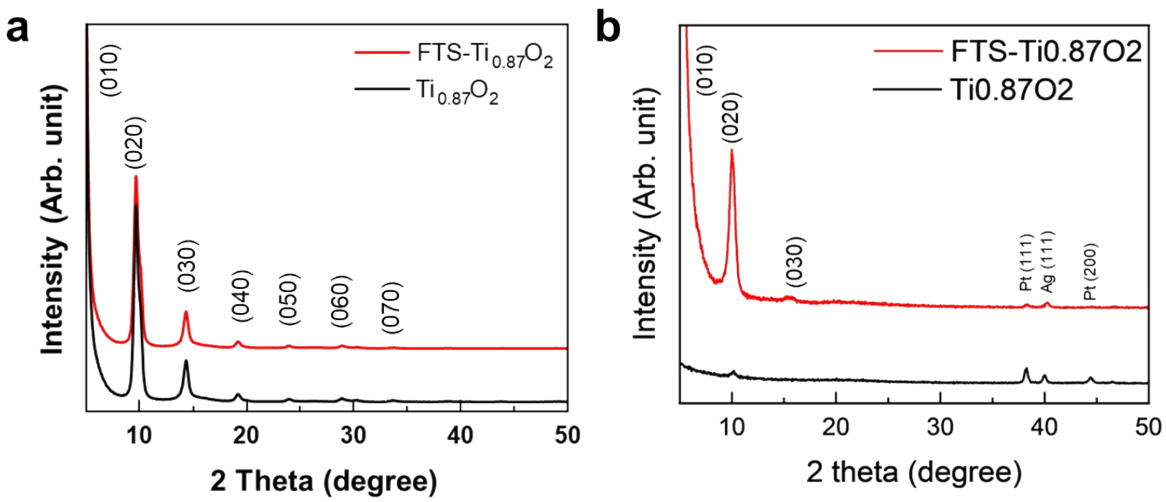

Fig S13. (a) XRD analysis of $Ti_{0.87}O_2$ and FTS-$Ti_{0.87}O_2$, and (b) after cycle test conditions, respectively

Fig S14. SEM images of $Ti_{0.87}O_2$ and FTS-$Ti_{0.87}O_2$: (a, b) before and (c, d) after cycle test conditions

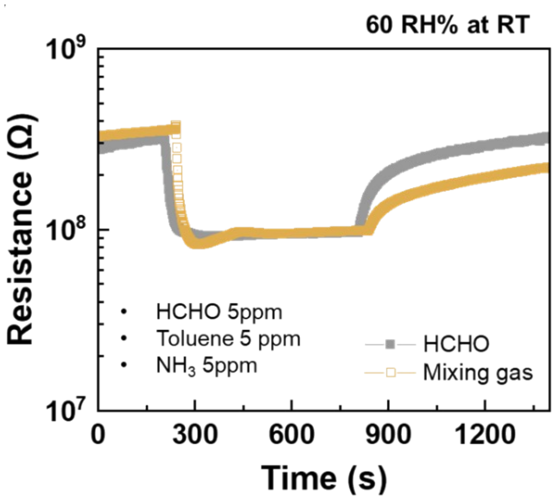

Fig. S15 Gas sensing properties of FTS-$Ti_{0.87}O_2$ of formaldehyde gas detection in various mixing gases (toluene, ammonia, formaldehyde)

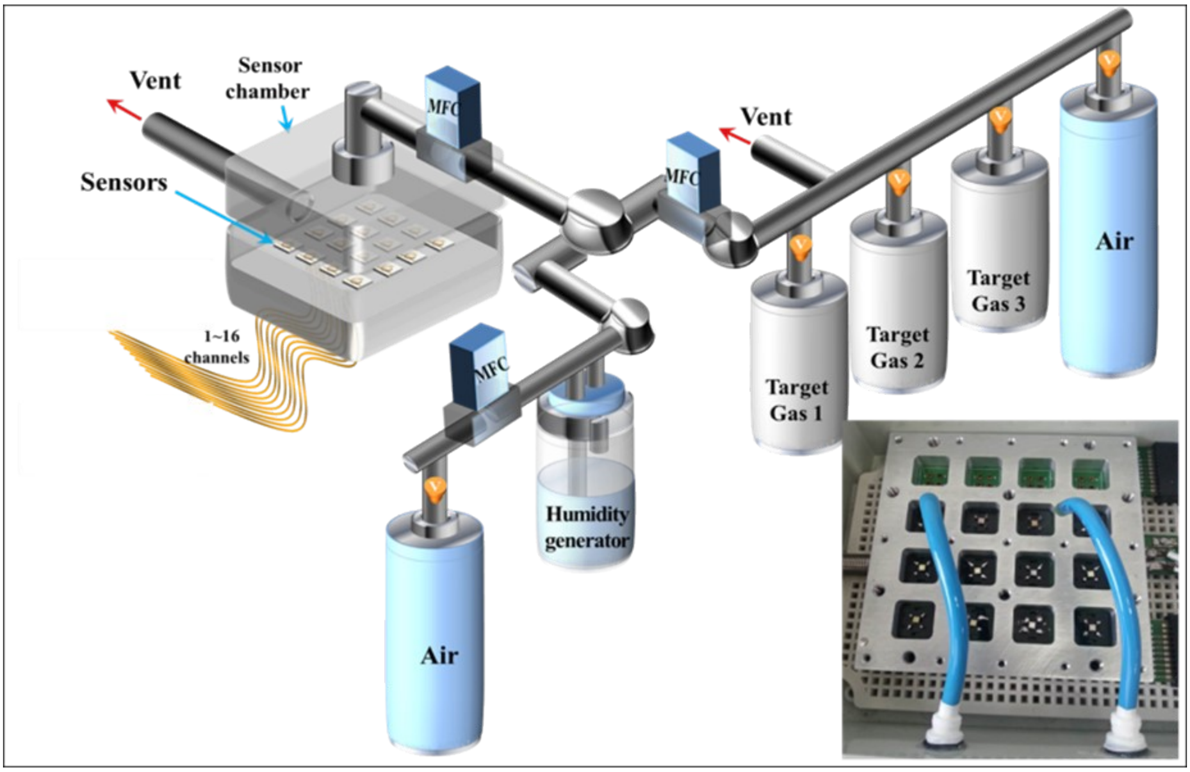

Fig. S16. The photo of the sensing system in working condition.

Table S1. Comparison of the sensing performance of HCHO sensors at room temperature

No.	Reference	Material	Structures	Concentration	Response	Response time	Limit of detect
This work		$Ti_{0.87}O_2$	Porous Nanosheet	5 ppm	213 %	97 s	99.13 ppb
1	J. Mater. Chem., 2012, 22, 12915-12920	In_2O_3/ZnO	Nanoflowers	5 ppm	19 %	-	5 ppm
2	Nanoscale 4 (2012) 5651–5658.	ZnO QDs/ graphene	Nanosheet	100 ppm	2.10 %	30 s	25 ppm
3	Appl. Phys. Lett. 105, 033107 (2014)	ZnO/graphene	Thin film	9 ppm	1.50 %	36 s	135 ppb
4	Sens. Actuators, B, 2015, 221, 1290–1298	ZnO/rGO	Nanoflowers	15 ppm	6 %	34 s	2 ppm
5	J. Electrochem. Soc., 2016, 163, B517	Au@ZnO	Nanosheet-sphere	5 ppm	10.57 %	13.8 s	1 ppm
6	Sens. Actuators, B 256 (2018) 1011–1020.	SnO_2/VG	Thin film	5 ppm	5.50 %	46 s	0.02 ppm
7	Microchemical Journal 160 (2021) 105607	ZnO-ANS-rGO	Nanosheet	5 ppm	1.05 %	300 s	5 ppm
8	Applied Surface Science 605 (2022) 154839	Au-In_2O_3 / $Ti_3C_2T_x$ Mxene	Nanosphere/ nanosheets	5 ppm	31 %	5 s	5 ppm
9	Materials Letters 350 (2023): 134927	$NiCo_2O_4$	Nanoneedles	50 ppm	1.85 %	22 s	10 ppm
10	Results in Chemistry 5 (2023) 100946	TiO_2	Thin film	20 ppm	85.87 %	35 s	1 ppm
11	Nature Communications (2021) 12:4955	MMM (ZIF-7/ PEBA) - coated TiO_2	Membrane	5 ppm	1350	57.4 s	3.8 ppb
12	Sci. Adv.10, eadk6856 (2024)	3D printed QDs/rGO	Aerogels	1 ppm	15.23%	< 30 s	8.02 ppb